Status of the Focal Plane Polarimeter for Hall A at TJNAF

M. K. Jones*, F. T. Baker‖, L. Bimbot‡, E. J. Brash††, R. Gilman‡, C. Glashausser‡, G. Kumbartzki‡, J. McIntyre‡, C. F. Perdrisat*, V. Punjabi†, G. Quéméner*, R. Ransome‡, P. M. Rutt‡, K. Wijesooriya*, G. D. Zainea††
and the TJNAF Hall A Collaboration.

*College of William and Mary, Williamsburg, VA 23187, USA
†Norfolk State University, Norfolk, VA 23504, USA
‡Rutgers University, Piscataway, NJ 08855, USA
‖Unviersity of Georgia, Athens, GA 30602, USA
††University of Regina, Regina, SK S4s 0A2, Canada

Abstract. The focal plane polarimeter (FPP) for Hall A at the Thomas Jefferson National Accelerator Facility (TJNAF) is ready for experiments. The ability to calibrate the FPP on-site using elastic scattering of polarized electrons from an unpolarized hydrogen target is demonstrated. The ratio of the proton electric form factor to its magnetic form factor has been measured at $Q^2 = 0.810\ (GeV/c)^2$.

INTRODUCTION

Intermediate-energy proton polarimeters are generally based on nuclear scattering of the proton from a carbon analyzer. Due to the spin-orbit force an azimuthal asymmetry is measured in the differential cross section. The focal-plane polarimeter (FPP), installed in the Fall of 1996 in one of the Hall A high resolution spectrometers at the Thomas Jefferson National Accelerator Facility (TJNAF), is unique in several aspects, in that it is physically large, makes use of straw tube drift chambers and multiplexing electronics, and is the second FPP to be operated at an electron accelerator.

PHYSICAL DESCRIPTION OF THE FPP

The FPP consists of two straw tube drift chambers in front and two straw tube drift chambers behind the carbon analyzer. The straw chamber design is based on a design originally created for the EVA cylindrical straw chamber, experiment E850 at Brookhaven National Laboratory [1]. The straw tubes were made by wrapping together 10 micron thick aluminum foil and two 50 micron thick mylar layers plus heat setting glue. The inner diameter of the straws is 0.522 cm.

The front chambers were constructed identically and each has three U planes and three V planes adding up to a total of 2016 straws. The U and V planes are perpendicular to each other and rotated 45 degrees from the x-axis. The x-direction is the dispersive direction and z is in the proton momentum direction. For both the U and V planes, the three layers of straws are arranged so that the middle row is offset by half a straw diameter and the bottom and top layers line up. The active area of the front chambers is 60 cm in the y-direction by 209 cm in the x-direction. The distance between the front chambers is 117 cm.

To track the particle after scattering in the carbon analyzer two straw tube chambers are used. The rear chamber closest to the carbon analyzer has two U planes, two V planes and two X planes with the planes offset by a straw radius. This chamber has an active area of 124 cm in the y-direction by 272 cm in the x-direction. The X planes are used in reconstructing multiple-track events. The second rear chamber is 42 cm behind the first rear chamber and it has three U planes and three V planes with the middle plane offset by a straw radius. This chamber has an active area of 135 cm in the y-direction by 290 cm in the x-direction. The total number of straws for the rear chambers is 2274. The distance between the second front chamber and the first rear chamber is 97 cm.

The carbon analyzer is divided into five moveable sections. The sections have thicknesses of 1.9 cm, 3.8 cm, 7.6 cm, 15.2 cm and 22.9 cm with the thickest one closest to the front chambers. The ability to vary the carbon thickness allows optimization of the FPP performance. The distance between the second front chamber and the front of the 22.9 cm carbon analyzer is 26.5 cm. The large size of the rear chambers allows detection of all events scattered in the carbon with through angles less than 20 degrees.

Given the large number of straws, multiplexing of the readout of the straw signals was imperative to reduce costs. The readout of the straw signals is multiplexed in groups of eight which would allow about 100 kHz rate capability per straw. The Rutgers University electronics shop built readout boards which were small enough to be located near the straws (reducing possible noise pick-up) and could still contain the circuitry for amplifying, discriminating and multiplexing the straw signals. The multiplexing is done by using discriminator one-shots with fixed widths that vary from 25 to 105 ns for each group of eight. Multi-hit TDCs are used to measure the leading and trailing

edge of the pulse. The leading edge determines the drift time and the difference between trailing and leading edges identifies the wire within the group of eight.

The gas used in the FPP chambers is a 62/38 mixture of argon/ethane. The threshold for the amplifier was set to correspond to chamber signals of about 2 μA. The efficiency of the chambers was measured to be 96%. Comparing FPP chamber tracks to those measured by the vertical drift chambers one can calculate the tracking efficiency of the FPP chambers to be 99%.

PRINCIPLES OF POLARIMETRY

The FPP will be used to measure the polarization of protons produced in electron and photon reactions. The components of outgoing proton polarization at the target are along the direction of the proton, P_z, in the dispersive direction, P_x, and in the transverse direction, P_y. While traveling through the spectrometer the proton polarization components at the target precess in the magnets. In the case of a simple dipole the proton polarization components at the focal plane (designated by a prime) are

$$P'_y = hP_y \quad P'_x = P_x \cdot \cos(\chi) - hP_z \cdot \sin(\chi) \tag{1}$$

In the equation χ is the spin precession angle and h is the beam helicity. The spectrometer's central bend angle is 45° for the Hall A dipole.

The FPP can only measure the transverse polarization components P'_x and P'_y but not the longitudinal component P'_z. The scattering of the proton in the carbon can be described in polar coordinates by scattering angles θ and ϕ. The ϕ-distribution can be made by summing over a range of θ. A ϕ-distribution which includes instrumental asymmetries would be

$$N(\phi) = N_o \cdot (1 + (a + a_i)\cos\phi + (b + b_i)\sin\phi + c_i\cos(2\phi) + d_i\sin(2\phi)) \tag{2}$$

$$a = -AP'_x \text{ and } b = AP'_y \tag{3}$$

where N_o is the average number of scattering events, A is the analyzing power of carbon and a_i, b_i, c_i and d_i are coefficients describing instrumental asymmetries.

For polarized electron scattering on a proton, $P_x \approx 0$. The other two components are

$$\begin{aligned} P_y &= -2\sqrt{\tau(1+\tau)}G_E^p G_M^p \tan(\frac{\theta_e}{2})/I_o \\ P_z &= \left(\frac{E_e + E_e^{'}}{M}\right)(G_M^p)^2\sqrt{\tau(1+\tau)}\tan^2(\frac{\theta_e}{2})/I_o \text{ with} \\ \tau = \frac{Q^2}{4M} &\text{ and } I_o = (G_E^p)^2 + \tau\,(G_M^p)^2\left[1 + 2(1+\tau)\tan^2(\frac{\theta_e}{2})\right] \end{aligned} \tag{4}$$

In the equations $E_e, E_e^{'}$, θ_e, M , Q^2 denote the incident electron energy, the scattered electron energy, the scattered electron angle, the mass of the proton and the momentum transfer squared [2,3]. G_E^p and G_M^p are the Sachs electric and magnetic form factors of the proton.

For the reaction ^{1}H($\vec{\text{e}}$,e'$\vec{\text{p}}$), Eq. 1 reduces to $P_y' = hP_y$ and $P_x' = -hP_z \sin(\chi)$. Therefore, the polarizations depend on the beam helicity which can be flipped between "plus" and "minus" states during the measurement. By taking the difference between ϕ-distributions, $N^+(\phi)$, gated on plus beam helicity, and $N^-(\phi)$, gated on minus beam helicity, one expects a ϕ-distribution

$$\begin{aligned} \frac{N^+(\phi)}{2N_o^+} - \frac{N^-(\phi)}{2N_o^-} &= a\cos(\phi) + b\sin(\phi) \\ a = -AP_x^{'} = hAP_z\sin(\chi) \;\text{ and }\; b &= AP_y^{'} = hAP_y \end{aligned} \tag{5}$$

Thus the instrumental asymmetries have been eliminated and only asymmetries from the physics are left. Combining Eq. 5 and Eq. 4, one can compute

$$\frac{G_E^p}{G_M^p} = \frac{P_y}{P_z}\frac{E_e + E_e^{'}}{M}\tan(\frac{\theta_e}{2}) = \frac{-b}{2a}\sin(\chi)\frac{E_e + E_e^{'}}{M}\tan(\frac{\theta_e}{2}) \tag{6}$$

in which the ratio $\frac{G_E^p}{G_M^p}$ is independent of beam helicity and the analyzing power of carbon. Also using a and b a second independent quantity

$$hA = \frac{a\left[\frac{b(E_e+E_e^{'})\sin(\chi)}{2aM}\right]^2 + \tau\left[\cot^2(\theta_e) + 2(1+\tau)\right]}{\frac{(E_e+E_e^{'})}{M}\sqrt{\tau(1+\tau)}\sin(\chi)} \tag{7}$$

can be calculated. Since the beam helicity is measured, the analyzing power of the carbon can be determined and the FPP can be calibrated at Hall A.

With the reaction ^{1}H($\vec{\text{e}}$,e'$\vec{\text{p}}$) the instrumental asymmetries of the FPP can be measured at the same time by taking the sum of the ϕ-distributions of plus and minus helicity beam (basically making the beam unpolarized). The ϕ-distribution can be described as

$$\frac{N^+(\phi)}{2N_o^+} + \frac{N^-(\phi)}{2N_o^-} = 1 + a_i\cos(\phi) + b_i\sin(\phi) + c_i\cos(2\phi) + d_i\sin(2\phi) \tag{8}$$

In this way the ratio of G_E^p to G_M^p, the analyzing power of carbon and the instrumental asymmetries of the FPP can be determined simultaneously.

TEST RESULTS

To test the FPP we measured the reaction ^{1}H($\vec{\text{e}}$,e'$\vec{\text{p}}$) at Q^2 of 0.810 $(GeV/c)^2$ where the ratio of G_E^p to G_M^p and the analyzing power of

carbon have been measured previously. The incident polarized electron beam had an energy of 2.4 GeV and a polarization of 37% which was flipped at a rate of 30 Hz. The electron scattering angle was 23.4 degrees. The scattered proton had a kinetic energy of 432 MeV. The average proton precession angle was 117.8 degrees. The target was a three-foil waterfall target. Scattering events from hydrogen were separated from oxygen events by a cut on the missing energy versus missing momentum histogram. Separate runs were taken with a carbon thickness of 15.2 and 22.9 cm. The ϕ-distributions were measured for θ between 5° and 20°.

In Figs. 1a and 1b the ϕ-distributions are shown for the plus helicity beam and the minus helicity beam. The ϕ-distributions are fitted by Eq. 2. The

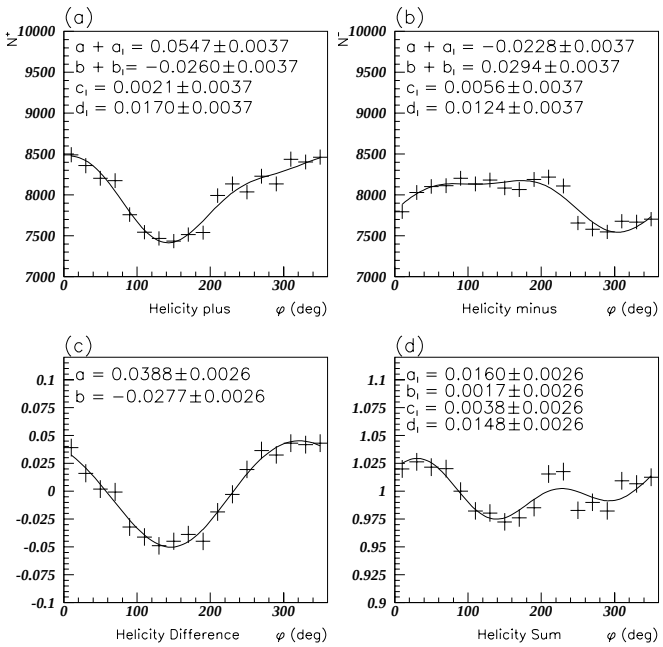

FIGURE 1. (a) The ϕ-distribution for plus helicity beam. (b) The ϕ-distribution for minus helicity beam. In (a) and (b) the line is a fit using Eq. 2. (c) The difference between the ϕ-distributions for the two beam helicity states. The line is a fit using Eq. 5. (d) The sum of the ϕ-distributions for the two beam helicity states. The line is a fit using Eq. 8.

ϕ-distribution for the sum of helicity states, as given by Eq. 8, is shown in Fig. 1d. The instrumental asymmetries are all less than 0.02. The design goal is to have instrumental asymmetries less than 0.005. An effort is underway to understand the origin of instrumental asymmetries and how they can be reduced.

The ϕ-distribution for the difference of helicity states, as given by Eq. 5, is shown in Fig. 1c. Using a and b determined by the fit with Eq. 5 one calculates $\mu G_E^p/G_M^p = 0.87 \pm 0.10$. When the data taken for the 22.9 cm

carbon thickness and the 15.2 cm data are combined in a weighted average, $\mu G_E^p/G_M^p = 0.92 \pm 0.09$ is determined. The value is in good agreement with previous measurements as shown in Fig. 2. The run time was short for this commissioning, thus the error on G_E^p/G_M^p is dominated by statistics. In practice the error can be reduced to 0.02 with a reasonable amount of running time. Using Eq. 7 the analyzing power of the carbon is 0.37 ± 0.018 which is

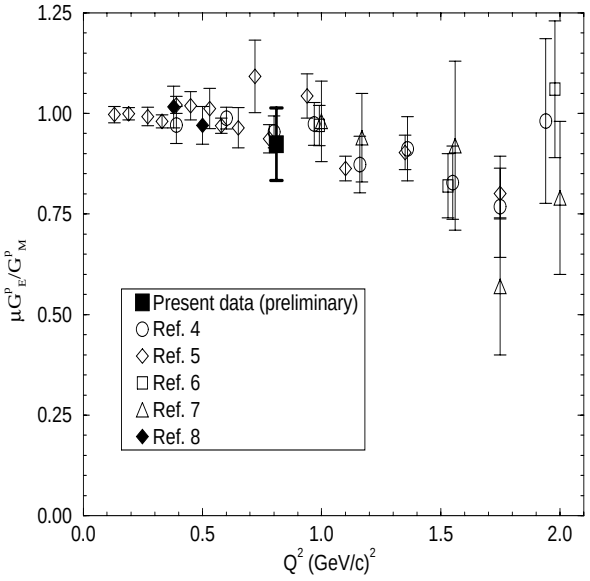

FIGURE 2. The ratio of $\mu G_E^p/G_M^p$ versus Q^2 All previous measurements were made using the Rosenbluth separation method [4–7], except for Ref. [8] which was the first to use a FPP to determine G_E^p/G_M^p.

in good agreement with the parametrization of Ref. [9] which gives a value of $0.36 \pm .007$. This result demonstrates that the FPP can be calibrated on-site.

CONCLUSIONS

Commissioning measurements using the FPP have shown that the detector can be calibrated on-site. Agreement with previous measurements of G_E^p/G_M^p demonstrate that the FPP is working properly and that corrections to the spin precession through the spectrometer from the simple dipole model are minimal. The FPP will be used in its first production experiment to measure the polarization components in the $^{16}\mathrm{O}(\vec{\mathrm{e}},\mathrm{e}'\vec{\mathrm{p}})$ reaction at electron beam energies of 2.4 GeV and recoil momenta from 85 MeV/c to 140 MeV/c. The next scheduled experiment at Hall A to use the FPP will measure G_E^p/G_M^p in

a Q^2 range between 0.5 to 3.0 $(\mathrm{GeV/c})^2$ with an accuracy of between 0.02 and 0.035.

REFERENCES

1. M. Kmit, M. Montag, A. S. Carroll, F. J. Barbosa, and S. H. Baker, Brookhaven Informal Report EP&S 91-4.
2. R. G. Arnold, C. E. Carlson, F. Gross, *Phys. Rev. C* **23**, 363 (1981).
3. A. I. Akhiezer and M. P. Rekalo, *Sov. J. Part. Nucl.* **4**, 277 (1974)
4. Ch. Berger, V. Burkert, G. Knop, B. Langenbeck and K. Rith, *Phys. Lett.* **35B**, 87 (1971).
5. L. E. Price, J. R. Dunning, M. Goiten, K. Hanson, T. Kirk and R. Wilson, *Phys. Rev. D* **4**, 45 (1971).
6. J. Litt *et al.*, *Phys. Lett.* **31B**, 40 (1970).
7. W. Bartel *et al.*, *Nucl. Phys.* **B58**, 429 (1973).
8. B. Milbrath *et al.*, submitted to Phys. Rev. Lett.
9. M. W. McNaughton *et al.*, *Nucl. Instr. Meth.* **A241**, 435 (1985).